Available online at www.sciencedirect.com
ScienceDirect
Trans. Nonferrous Met. Soc. China 23(2013) 2066−2070
Transactions of Nonferrous Metals Society of China
www.tnmsc.cn

Effects of chromium doping on performance of $LiNi_{0.5}Mn_{1.5}O_4$ cathode material

Wei WANG[1], Heng LIU[1], Yan WANG[2], Chao GAO[1], Jun ZHANG[1]

1. College of Materials Science and Engineering, Sichuan University, Chengdu 610065, China;
2. College of Computer Science and Technology, Southwest University for Nationalities, Chengdu 610041, China

Received 21 July 2012; accepted 26 November 2012

Abstract: In order to improve the cycle and rate performance of $LiNi_{0.5}Mn_{1.5}O_4$, $LiCr_{2Y}Ni_{0.5-Y}Mn_{1.5-Y}O_4$ ($0\leq Y\leq 0.15$) particles were synthesized by the sucrose-aided combustion method. The effects of Cr doping in $LiNi_{0.5}Mn_{1.5}O_4$ on the structures and electrochemical properties were investigated. The samples were characterized by X-ray diffractometry (XRD), scanning electron microscopy (SEM), cyclic voltammetry (CV), galvanostatic charge-discharge test and electrochemical impedance spectrum (EIS). The results indicate that the $LiCr_{2Y}Ni_{0.5-Y}Mn_{1.5-Y}O_4$ possess a spinel structure and small particle size, and $LiCr_{0.2}Ni_{0.4}Mn_{1.4}O_4$ exhibits the best cyclic and rate performance. It can deliver discharge capacities of 143 and 104 mA·h/g at 1*C* and 10*C*, respectively, with good capacity retention of 96.5% at 1*C* after 50 cycles.
Key words: lithium ion batteries; cathode material; spinel; Cr doping; lithium nickel manganese oxide

1 Introduction

Recently, the spinel material $LiNi_{0.5}Mn_{1.5}O_4$ has been intensively studied because of its low cost, low toxicity, abundant raw materials and good electrochemical performance [1−4]. It becomes the 3rd generation lithium-ion cathode material [5] after $LiCoO_2$, $LiMn_2O_4$ and $LiFePO_4$. This material has especially attracted attention because of its high practical voltage of 4.7 V. The high working voltage can lead to a high energy density, so the batteries with this material as cathode will produce a high energy output, which makes it the most attractive material for practical use [6].

However, it has been reported that the cycling behavior of spinel $LiNi_{0.5}Mn_{1.5}O_4$ material is not satisfactory [7]. The structural and electrochemical properties of the $LiNi_{0.5}Mn_{1.5}O_4$ could also be affected by the substitution of other metal ions. It will be promising if proper cation doping can be used in spinel $LiNi_{0.5}Mn_{1.5}O_4$ to further improve its electrical conductivity. So far, some researches about doping elements such as Fe, Al, Ru, Cr and Ti have been reported [8]. Among them, Cr-doped material could be used in high rate lithium-ion batteries due to the super cycling performance at high rates [9−12].

In this study, the effects of doping Cr content on the performance of $LiNi_{0.5}Mn_{1.5}O_4$ cathode material were studied. Several Cr-doped samples with general formula $LiCr_{2Y}Ni_{0.5-Y}Mn_{1.5-Y}O_4$ ($0\leq Y\leq 0.15$) were synthesized by combustion method. And a small particle size and a high rate capacity were expected for these cathode materials.

2 Experimental

The high-voltage spinel $LiCr_{2Y}Ni_{0.5-Y}Mn_{1.5-Y}O_4$($Y$=0, 0.05, 0.1 and 0.15) was synthesized by the sucrose-aided combustion method. Stoichiometric amounts of $LiNO_3$, $Cr(NO_3)_3\cdot 9H_2O$, $Ni(NO_3)_2\cdot 4H_2O$ and $Mn(CH_3COO)_2\cdot 4H_2O$ (Changzheng Chemical, Chengdu) were used as starting materials, and sucrose(mole ratio of sucrose to the product being 1:1) as fuel. In order to compensate for the loss of Li during heating at high reaction temperatures, approximately 5% of additional Li salt was made up. At first, the starting materials were dissolved in distilled water and stirred for some time. After being dissolved in the minimum amount of distilled water, sucrose was added to the mixed solution. The mixed solution was evaporated for a while until the water was removed as far as possible at 100 °C. Then the mass

Foundation item: Project (2007BA201055) supported by the National Science and Technology Support Program, China
Corresponding author: Heng LIU; Tel: +86-28-85410272; E-mail: h_liu@scu.edu.cn
DOI: 10.1016/S1003-6326(13)62697-7

was transferred to an oven at 150 °C for removing some of volatile. The precursors were first calcined at 500 °C for 1 h, and cooled down to room temperature. Then the intermediate products were ground in an agate and sintered at 900 °C for 1 h in air, and the heating/cooling rate was 2 °C/min.

Powder X-ray diffraction (Philips) using Cu K_α radiation was used to identify the crystalline phase of the materials. The particle size and morphology were studied by a scanning electron microscope (JSM−5900LV, JEOL).

The electrochemical properties of the $LiCr_{2Y}Ni_{0.5-Y}Mn_{1.5-Y}O_4$ were tested by lithium half-cell. The cathode was prepared by casting the slurry of 72% active material, 20% acetylene black, and 8% PVDF binder in NMP on an aluminum foil, and drying at 80 °C overnight. CR2032 coin cells were assembled with Li metal foil as anode and 1 mol/L $LiPF_6$ in EC: DMC (1:1 in volume ratio) as electrolyte in an argon glove box. The cells were galvanostatically cycled on a multi-channel battery cycler (Neware, Shenzhen, China) in the range of 3.4−5.2 V. All the tests were carried out at room temperature. The cyclic voltammetry (CV) tests and electrochemical impedance spectroscopy (EIS) were performed on an electrochemical workstation (CHI660B).

3 Results and discussion

3.1 Structural and morphological characterization

The XRD patterns of the spinel powders are shown in Fig. 1. It can be clearly observed from the four samples that the diffraction peaks are sharp and the half-peak width is narrow, indicating that they have high degree of crystallinity. The results reveal that the spinel structure was well maintained and there were no impurity phases such as NiO and $Li_xNi_{1-x}O$, which were reported in Refs. [13,14]. The structures are assigned to either face-centered spinel (*Fd*3*m*) or primitive simple cubic crystal (*P*4332) which depends on the ordering of transition metal cations. For *P*4332 space group, the Ni^{2+} and Mn^{4+} transition metals occupy the 4a and 12d lattice positions, respectively. The oxygen ions occupy the 24e and 8c positions, while the lithium ions are located in the 8c sites. For *Fd*3*m* space group, the lithium ions are located in tetrahedral 8a sites and transition metal elements fill the 16d octahedral sites. $LiCr_{2Y}Ni_{0.5-Y}Mn_{1.5-Y}O_4$ with disordered *Fd*3*m* shows better rate-ability than ordered *P*4332 spinels due to the higher electronic and ionic conductivities [15,16]. However, the structure difference between these two space groups can hardly be observed by XRD. In the *Fd*3m space group, there are both Mn^{3+} and Mn^{4+},while in the *P*4332 space group, all Mn ions are Mn^{4+} [17]. The voltage plateau at about 4 V resulted from Mn^{3+}/Mn^{4+} in the subsequent charge–discharge curves indicates the presence of Mn^{3+}. So, it can be concluded that the as-prepared materials have a cubic spinel structure with *Fd*3*m* space group.

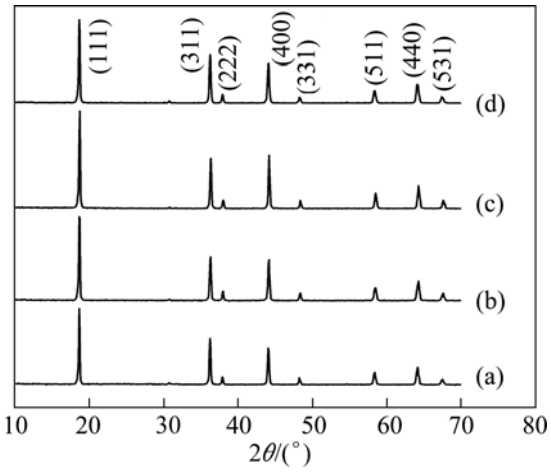

Fig. 1 XRD patterns of $LiNi_{0.5}Mn_{1.5}O_4$ (a), $LiCr_{0.1}Ni_{0.45}Mn_{1.45}O_4$ (b), $LiCr_{0.2}Ni_{0.4}Mn_{1.4}O_4$ (c) and $LiCr_{0.3}Ni_{0.35}Mn_{1.35}O_4$ (d)

The lattice parameters for samples shown in Figs. 1(a), (b), (c) and (d) are 8.2083, 8.1966, 8.1927 and 8.2098 Å, respectively. The ion radii for Mn^{4+}, Ni^{2+} and Cr^{3+} are 0.6, 0.69 and 0.63 Å, respectively. So, when $LiNi_{0.5}Mn_{1.5}O_4$ is doped with appropriate Cr, the Mn and Ni ions of unit cell are replaced partially by Cr^{3+}, resulting in the shrinkage of unit cell and volume decrease. But when Cr is excessive, some extra Cr^{3+} may replace the position of Mn^{4+} instead of Ni^{2+}, making the lattice parameter increase. The smaller crystal parameter contributes to the more stable crystal structure of material, and cycling and rate performance of the materials and expected to be improved obviously.

Figure 2 shows the SEM images of the $LiNi_{0.5}Mn_{1.5}O_4$ and the Cr-doped samples. Smaller particles can shorten the diffusion pathway of lithium ion in charge−discharge test. It can be observed that the particle morphologies of these samples are almost the same angular spinel shape. All samples present the similar submicron size particles, which could explain that sucrose plays a role in mixing solution more uniform and separating the particles at the mixed stage of raw materials so as to make dried precursor particles much finer. In addition, the steric hindrance effect formed among grains by released gases during the combustion can prevent the excessive growth of particle size [18].

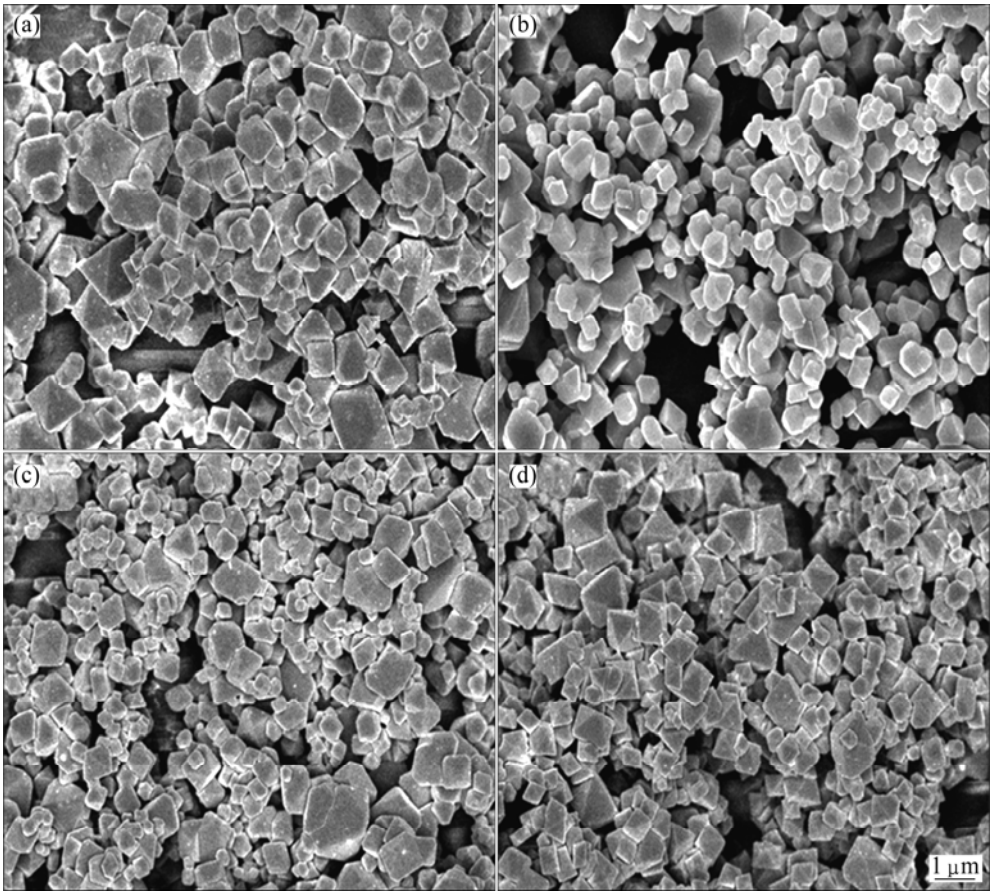

Fig. 2 SEM images of samples $LiNi_{0.5}Mn_{1.5}O_4$ (a), $LiCr_{0.1}Ni_{0.45}Mn_{1.45}O_4$ (b), $LiCr_{0.2}Ni_{0.4}Mn_{1.4}O_4$ (c) and $LiCr_{0.3}Ni_{0.35}Mn_{1.35}O_4$ (d)

3.2 Electrochemical properties

Figure 3 shows the cyclic voltammograms (CV) of the $LiNi_{0.5}Mn_{1.5}O_4$ and the Cr-doped samples in the voltage ranging from 3.4 to 5.2 V with a scan rate of 0.1 mV/s. All the four samples show three well-defined peaks at about 4.0, 4.6 and 4.7 V in discharge, which correspond to Mn^{3+}/Mn^{4+}, Ni^{2+}/Ni^{3+} and Ni^{3+}/Ni^{4+} redox couples, but for the Cr-doped samples (curves (b), (c) and (d), there are extra peaks at around 4.9 V, which are assigned to Cr^{3+}/Cr^{4+} redox couple. Furthermore, when Cr-content is as high as 0.3, the intensity of peak at 4.9 V is the strongest. Meanwhile, the intensities of peaks at 4.6 and 4.7 V are the weakest due to the reduction of Ni and Mn contents. So, the CV curves match the samples with different formulas very well.

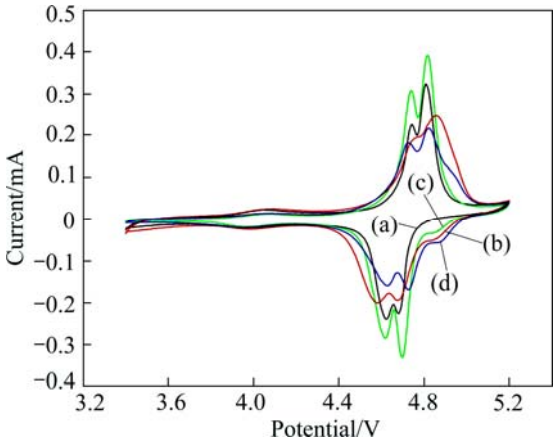

Fig. 3 Cyclic voltammograms of $LiNi_{0.5}Mn_{1.5}O_4$ (a), $LiCr_{0.1}Ni_{0.45}Mn_{1.45}O_4$ (b), $LiCr_{0.2}Ni_{0.4}Mn_{1.4}O_4$ (c) and $LiCr_{0.3}Ni_{0.35}Mn_{1.35}O_4$ (d)

Figure 4 shows the 2nd charge-discharge cyclic curves of the $LiNi_{0.5}Mn_{1.5}O_4$ and the Cr-doped samples in the voltage ranging from 3.4 to 5.2 V. Charge−discharge tests were carried out at 0.5*C* and 1*C* rates, respectively. It can be found that there are about three discharge plateaus in all the four samples except for $LiNi_{0.5}Mn_{1.5}O_4$. The first plateau is at about 4.0 V, and ascribed to Mn^{3+}/Mn^{4+} redox reaction. Two other plateaus are at about 4.7 and 4.9 V, and are assigned to Ni^{2+}/Ni^{4+} and Cr^{3+}/Cr^{4+} redox couples. For Cr-free $LiNi_{0.5}Mn_{1.5}O_4$ sample, its initial discharge plateau is lower than other three Cr-doped samples, which is consistent with the CV results.

Figure 5 demonstrates the discharge capacity of the samples at different *C*-rate after 2 cycles. The $LiCr_{0.2}Ni_{0.4}Mn_{1.4}O_4$ spinel presents the best electrochemical performance, and it can deliver a capacity of 143 mA·h/g at 1*C* rate. $LiNi_{0.5}Mn_{1.5}O_4$,

$LiCr_{0.1}Ni_{0.45}Mn_{1.45}O_4$ and $LiCr_{0.3}Ni_{0.35}Mn_{1.35}O_4$ have lower capacities of about 127, 129 and 127 mA·h/g, respectively. The sample $LiCr_{0.2}Ni_{0.4}Mn_{1.4}O_4$ gives a good cyclic and rate performance, with the discharge capacity slightly decreasing from 143 to 138 mA·h/g after 50 cycles, and the capacity retention is 96.5%. When the discharge rate reaches 10*C*, the $LiCr_{0.2}Ni_{0.4}Mn_{1.4}O_4$ material can still deliver a capacity of 104 mA·h/g, the highest capacity among all the four samples.

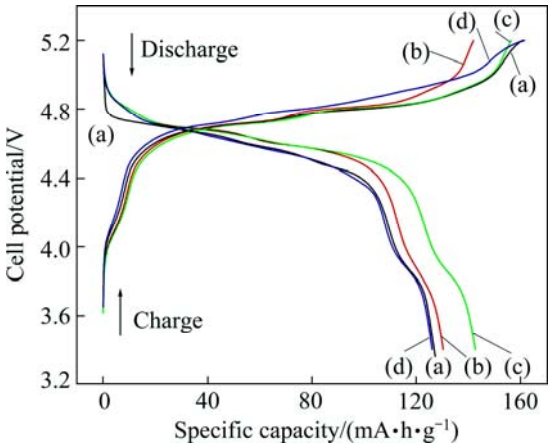

Fig. 4 The 2nd charge−discharge profiles of cells made of $LiNi_{0.5}Mn_{1.5}O_4$ (a), $LiCr_{0.1}Ni_{0.45}Mn_{1.45}O_4$ (b), $LiCr_{0.2}Ni_{0.4}Mn_{1.4}O_4$ (c) and $LiCr_{0.3}Ni_{0.35}Mn_{1.35}O_4$ (d)

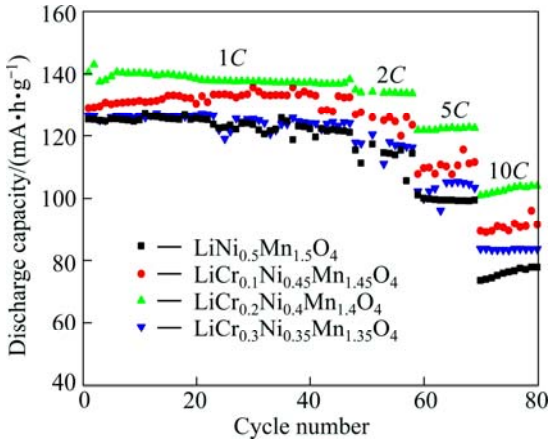

Fig. 5 Rate performance of $LiNi_{0.5}Mn_{1.5}O_4$ and Cr-doped spinels at various rates

It is known to all that the bonding energy of Cr—O is stronger than that of Mn—O or Ni—O. The stronger Cr—O bond is in favor of maintaining the spinel structure during cycling, and then prevents the structural disintegration of the material [19]. However, the presence of Mn^{3+} would tend to cause Mn dissolution and hence capacity fade. Cr doping stabilizes the crystal structure and tends to suppress the Mn dissolution. When Cr content is excessive, the structure might be changed a lot. And for this experiment, $LiCr_{0.2}Ni_{0.4}Mn_{1.4}O_4$ reveals the best rate performance at different discharge rates.

Electrochemical impedance spectrum (EIS) for the discharged cell was measured in the frequency ranging from 100 kHz to 10 MHz. As shown in Fig. 6, all spectra consist of a semicircle in the high frequency range and a sloping line at the low frequency range, being ascribed to the charge transfer resistance resulting from electrode reaction and the Warburg impedance caused by diffusion of lithium ion. An equivalent circuit model of EIS is constructed to analyze the resistance of $LiCr_{2Y}Ni_{0.5-Y}Mn_{1.5-Y}O_4$ electrode which can explain the impedance spectra through the surface resistance (R_s) and charge transfer resistance (R_{ct}). The fitting results are summarized in Table 1. As can be seen from Table 1, R_s of the four samples is nearly the same, but the charge transfer resistance for $LiCr_{0.2}Ni_{0.4}Mn_{1.4}O_4$ is only 189 Ω, indicating that its electrochemical polarization is the lowest and this kind of material has high electronic conductivity, which contributes to improving the cyclic and rate performance of the product, and it turns out that $LiCr_{0.2}Ni_{0.4}Mn_{1.4}O_4$ has the optimum electrochemical performance among all the four samples.

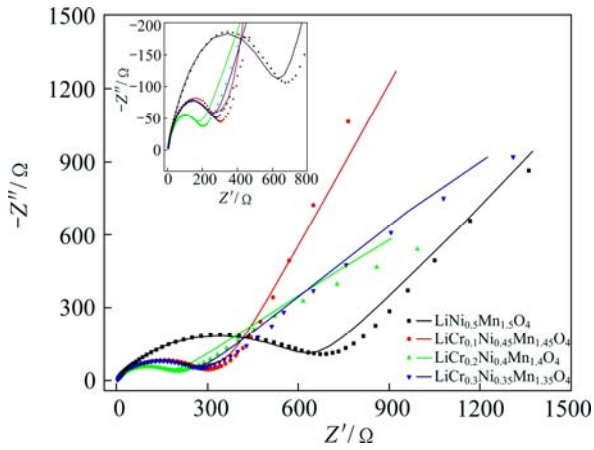

Fig. 6 EIS of $LiNi_{0.5}Mn_{1.5}O_4$ and Cr-doped spinel electrodes after 50 cycles at 1*C* (The inset graph is magnified EIS below 800 Ω framed in rectangle; point stands for initial data and line means fitting curve)

Table 1 Impedance parameters calculated from equivalent circuit

Sample	R_s/Ω	R_{ct}/Ω
$LiNi_{0.5}Mn_{1.5}O_4$	3.1575	685
$LiCr_{0.1}Ni_{0.45}Mn_{1.45}O_4$	3.2623	299
$LiCr_{0.2}Ni_{0.4}Mn_{1.4}O_4$	3.5643	189
$LiCr_{0.3}Ni_{0.35}Mn_{1.35}O_4$	3.2896	249

4 Conclusions

$LiNi_{0.5}Mn_{1.5}O_4$ and Cr-doped $LiCr_{2Y}Ni_{0.5-Y}Mn_{1.5-Y}O_4$ ($0 \le Y \le 0.15$) were synthesized by the sucrose-aided

combustion method. The as-prepared products have cubic spinel structures with *Fd*3*m* space group. Sample $LiCr_{0.2}Ni_{0.4}Mn_{1.4}O_4$ exhibits the best cyclic and rate performance. It can deliver discharge capacities of 143 and 104 mA·h/g at 1*C* and 10*C*, respectively, with good capacity retention of 96.5% at 1*C* after 50 cycles. This preparation method is easy to be implemented in industrial production because of its simple steps, short synthesis time and low energy consumption.

References

[1] WU Xiang-lan, KIM S B. Improvement of electrochemical properties of $LiNi_{0.5}Mn_{1.5}O_4$ spinel [J]. Journal of Power Sources, 2002, 109(1): 53−57.

[2] HONG K J, SUN Y K. Synthesis and electrochemical characteristics of $LiCr_XNi_{0.5-X}Mn_{1.5}O_4$ spinel as 5 V cathode materials for lithium secondary batteries [J]. Journal of Power Sources, 2002, 109(2): 427−430.

[3] YASUSHI L, HIROSUKE N, NOBUYUKI K. Crystal structure and cathode performance dependence on oxygen content of $LiNi_{0.5}Mn_{1.5}O_4$ as a cathode material for secondary lithium batteries [J]. Journal of Power Sources, 2003, 119−121(1): 125−129.

[4] ALCANTARA R, JARABA M, LAVELA P. Optimizing preparation condition for 5 V electrode performance, and structural changes in $Li_{1-X}Ni_{0.5}Mn_{1.5}O_4$ spinel [J]. Electrochimica Acta, 2002, 47(11): 1829−1835.

[5] LIN Chih-yuan, DUH Jeng-gong, HSU Chia-haw, CHEN Jin-ming. $LiNi_{0.5}Mn_{1.5}O_4$ cathode material by low-temperature solid-state method with excellent cycleability in lithium ion battery [J]. Materials Letters, 2010, 64(21): 2328−2330.

[6] WU H M, TU J P, YUAN Y F, LI Y, ZHAO X B, CAO G S. Structural, morphological and electrochemical characterisitics of spinel $LiMn_2O_4$ prepared by spray-drying method [J]. Scripta Materialia, 2005, 52(6): 513−517.

[7] ARUNKUMAR T A, MANTHIRAM A. Influence of chromium doping on the electrochemical performance of the 5 V spinel cathode $LiMn_{1.5}Ni_{0.5}O_4$ [J]. Electrochimica Acta, 2005, 50: 5568−5572.

[8] YI Ting-feng, XIE Ying, YE Ming-fu, JIANG Li-juan, ZHU Rong-sun, ZHU Yan-rong. Recent developments in the doping of $LiNi_{0.5}Mn_{1.5}O_4$ cathode material for 5 V lithium-ion batteries [J]. Ionics, 2011, 17(5): 383−389.

[9] LIU G Q, WEN L, LIU Y M. Spinel $LiNi_{0.5}Mn_{1.5}O_4$ and its derivatives as cathodes for high-voltage Li-ion batteries [J]. J Solid State Electrochem, 2010, 14(12): 2191−2202.

[10] AKLALOUCH M, AMARILLA J M, ROJAS R M, SAADOUNE I, ROJO J M. Sub-micrometric $LiCr_{0.2}Ni_{0.4}Mn_{1.4}O_4$ spinel as 5 V-cathode material exhibiting huge rate capability at 25 and 55 °C [J]. Electrochem Commun, 2010, 12(4): 548−552.

[11] PARK S B, EOM W S, CHO W I, JANG H. Electrochemical properties of $LiNi_{0.5}Mn_{1.5}O_4$ cathode after Cr doping [J]. Journal of Power Sources, 2006, 159(1): 679−684.

[12] AKLALOUCH M, AMARILLA J M, ROJAS R M, SAADOUNE I, ROJO J M. Chromium doping as a new approach to improve the cycling performance at high temperature of 5 V $LiNi_{0.5}Mn_{1.5}O_4$-based positive electrode [J]. Journal of Power Sources, 2008, 185(1): 501−511.

[13] ZHONG Qi-ming, BONAKDARPOUR A, ZHANG Mei-jie, GAO Yuan, DAHN J R. Synthesis and electrochemistry of $LiNi_XMn_{2-X}O_4$ [J]. Electrochem Soc, 1997, 144(1): 205−213.

[14] JIN Yi-chun, DUH Jengq-gong. Nanostructured $LiNi_{0.5}Mn_{1.5}O_4$ cathode material synthesized by polymer-assisted co-precipitation method with improved rate capability [J]. Materials Letters, 2013, 93(15): 77−80.

[15] KUNDURACI M, AMATUCCI G G. The effect of particle size and morphology on the rate capability of 4.7 V $LiMn_{1.5+\delta}Ni_{0.5-\delta}O_4$ spinel lithium-ion battery cathodes [J]. Electrochim Acta, 2008, 53(12): 4193−4199.

[16] KUNDURACI M, AL-SHARAB J F, AMATUCCI G G. High-power nanostructured $LiMn_{2-X}Ni_XO_4$ high-voltage lithium-ion battery electrode materials: Electrochemical impact of electronic conductivity and morphology [J]. Chemistry of Materials, 2006, 18(15): 3585−3592.

[17] KIM J H, MYUNG S T, YOON C S, KANG S G, SUN Y K. Comparative study of $LiNi_{0.5}Mn_{1.5}O_{4-\delta}$ and $LiNi_{0.5}Mn_{1.5}O_4$ cathodes having two crystallographic structures: *Fd*3*m* and *P*4332 [J]. Chemistry of Materials, 2004, 16(5): 906−914.

[18] LI Yuan. Research on the preparation and performance of high-voltage cathode material $LiCr_{0.2}Ni_{0.4}Mn_{1.4}O_4$as cathode materials for lithium ion battery [D]. Chengdu: Sichuan University, 2012: 26−30. (in Chinese)

[19] LIU Guo-qiang, XIE Hong-wei, LIU Li-ying, KANG Xiao-xue, TIAN Yan-wen, ZHAI Yu-chun. Synthesis and electrochemical performances of spinel $LiCr_{0.1}Ni_{0.4}Mn_{1.5}O_4$ compound [J]. Materials Research Bulletin, 2007, 42(11): 1955−1961.

掺铬对 $LiNi_{0.5}Mn_{1.5}O_4$ 正极材料性能的影响

王 巍[1]，刘 恒[1]，王 燕[2]，高 超[1]，张 军[1]

1. 四川大学 材料科学与工程学院，成都 610065；
2. 西南民族大学 计算机科学与技术学院，成都 610041

摘 要：为了改善 $LiNi_{0.5}Mn_{1.5}O_4$ 材料的循环和倍率性能，以蔗糖为助燃剂合成 $LiCr_{2Y}Ni_{0.5-Y}Mn_{1.5-Y}O_4$($0\le Y\le 0.15$)颗粒，并研究掺铬对 $LiNi_{0.5}Mn_{1.5}O_4$ 结构和电化学性能的影响。通过 X 射线衍射(XRD)、扫描电镜(SEM)、循环伏安(CV)、恒电流充放电测试和交流阻抗谱(EIS)对样品进行表征。结果表明，所制备材料呈现尖晶石结构并具有小颗粒尺寸，$LiCr_{0.2}Ni_{0.4}Mn_{1.4}O_4$ 表现出最佳的循环和倍率性能，在 1*C* 和 10*C* 倍率下的放电比容量分别为 143 和 104 mA·h/g，并且在 1*C* 倍率下循环 50 次后仍具有 96.5%的容量保持率。

关键词：锂离子电池；正极材料；尖晶石；掺铬；锂镍锰氧化物

(Edited by Xiang-qun LI)